Supplemental data for "**Elucidating inter-nucleosome interactions and their roles of histone tails**"

Steven C. Howell[1], Kurt Andresen[2], Isabel Jimenez-Useche[3], Chongli Yuan[3], and Xiangyun Qiu[1,*]

[1] Department of Physics, George Washington University, Washington, DC, 20052, USA;
[2] Department of Physics, Gettysburg College, Gettysburg, PA, 17325, USA;
[3] School of Chemical Engineering, Purdue University, West Lafayette, IN, 47907, USA
* To whom correspondence should be addressed. Tel: 001.202.994.6537; Fax: 001.202.994.3001; Email: xqiu@gwu.edu

I. Supporting data to the results presented in the main text

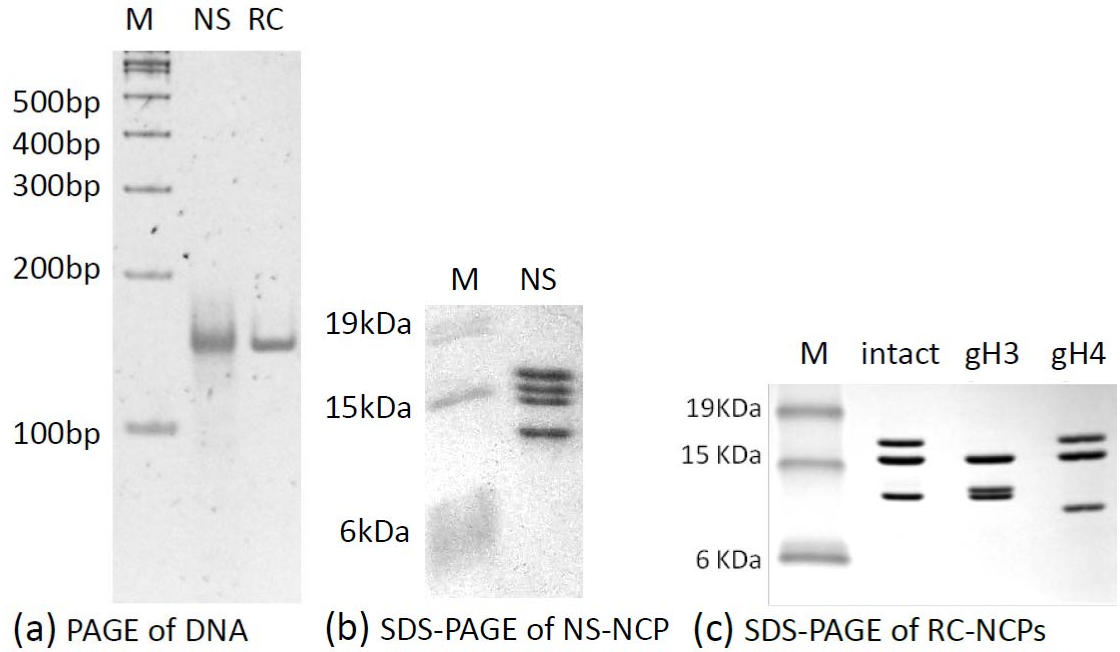

Figure S1. Characterization of nucleosome samples. (a) Extracted DNA from natural-source (NS) nucleosomes and the recombinant (RC) 147-base-pair (bp) mouse mammary tumor virus DNA in 5% polyacrylamide gel electrophoresis (PAGE). The "M" lane is the 100-bp DNA marker (Invitrogen). By analyzing the intensity distribution of each band, we obtained the full widths at half maximum (FWHM) of the bands in unit of pixels as, 100-bp marker: 10, 200-bp marker: 7.5, NS-DNA: 15, RC-DNA: 10.5. Given the distance between 100-bp and 200-bp markers are ~100 pixels, the additional smearing of the NS-DNA band is estimated to be ~10 pixels in FWHM, corresponding to ±5 base pairs. The maximum peak positions for NS-DNA and RC-DNA are identical within experimental error, noting that the NS-DNA band intensity

distribution is skewed toward longer DNA lengths as expected from the nucleosomal hindrance of Micrococcal nuclease digestion. We thus estimated the NS-DNA to be 147±5 bps. (b) Sodium dodecyl sulfate polyacrylamide gel electrophoresis (SDS-PAGE, 15%) of natural-source NCP histones. The "M" lane is the protein marker (Invitrogen BenchMark^{TM}). (c) SDS-PAGE of recombinant NCP histones ("intact" refers to the RC-NCP with all histone tails). Note that the recombinant H2A and H2B histones migrate as one band, while the H2A and H2B histones from NS-NCPs are well separated (b). Possible explanations include sequence differences and post-translational modifications in NS-NCP histones only.

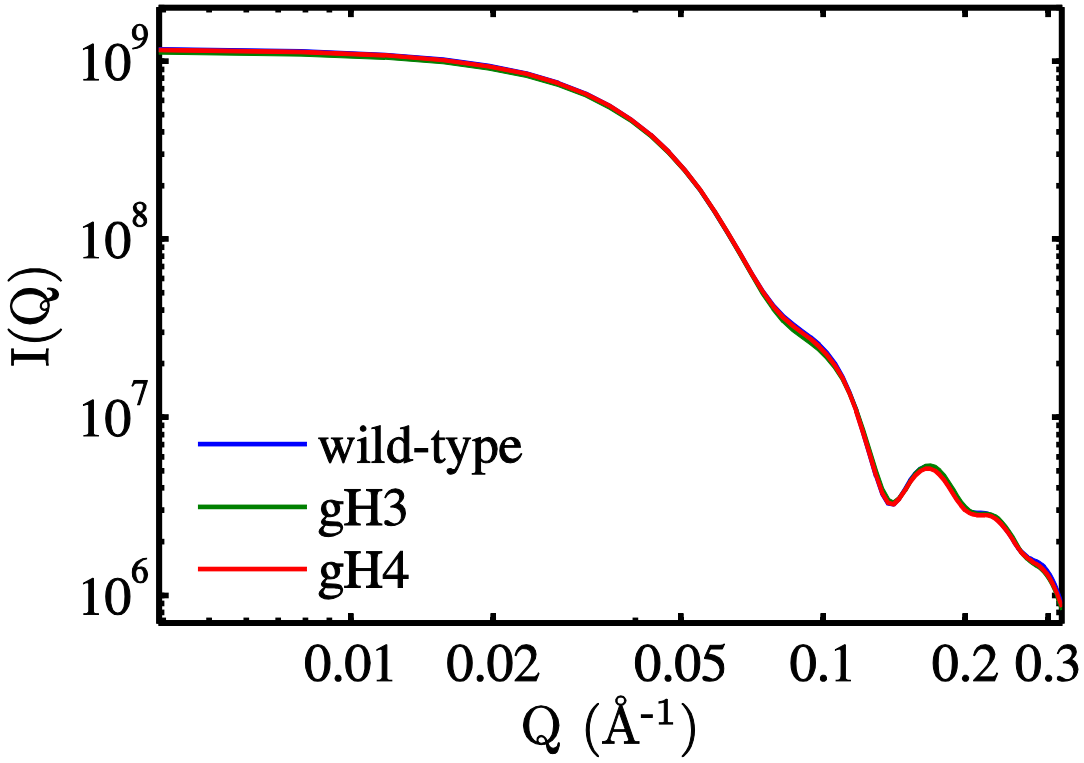

Figure S2. The form factors for the nucleosome constructs in this study. The SAXS profiles are calculated based on the nucleosome crystal structure (1KX5) using Crysol [1]. Atomic structures for the histone-tail-deletion constructs (i.e., gH3 and gH4 NCPs) are obtained by manual removal of the residues in accord with the constructs. The wild-type curve is used as the form factor for the NS-NCP and RC-NCP (results from the latter are shown in Suppl. Fig. S5). Comparisons of the three form factors indicate that tail deletions lead to rather small changes to the shape of the SAXS profile.

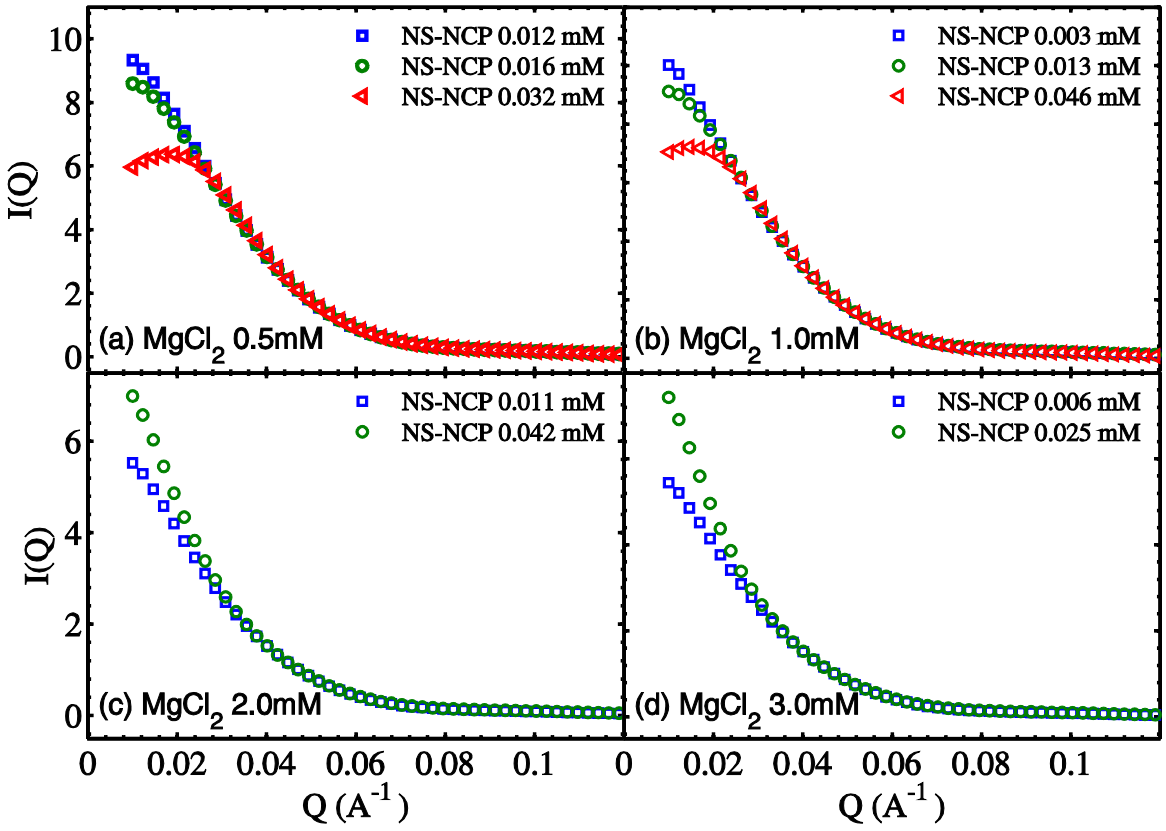

Figure S3. SAXS profiles of NS-NCPs in a series of $MgCl_2$ concentrations (no theoretical fits). Inter-NCP repulsions (low Q downturn) were observed at 0.5 and 1.0 mM $MgCl_2$, while attractions (low Q upturn) were observed at 2.0 and 3.0 mM $MgCl_2$. We have not been able to obtain satisfactory fits to the full SAXS profiles in Mg^{2+} salts using the Generalized One Component Method (GOCM). We do not yet know the reasons. One speculation is that the short-range inter-NCP interactions become strongly anisotropic in Mg^{2+} salts and the GOCM fails, or that there exist oligomeric states of NCPs in the presence of Mg^{2+}. Still, the qualitative observations of inter-NCP interactions (i.e., repulsion vs attraction) hold. Quantitative modeling of the SAXS data in Mg^{2+} salts is being actively pursued in our groups.

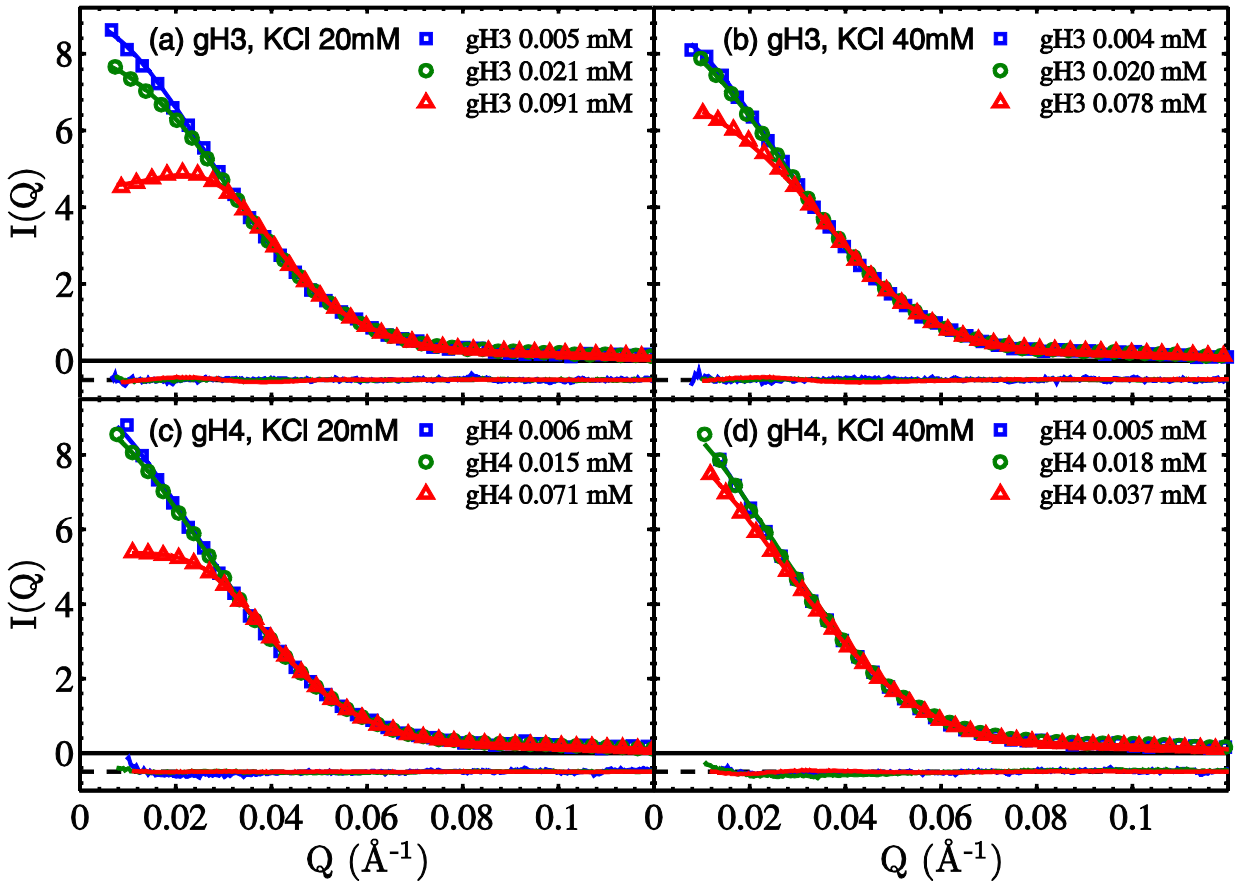

Figure S4. SAXS profiles and GOCM fits of gH3 and gH4 RC-NCPs at 20 and 40 mM KCl. I(Q)s are normalized by NCP concentrations to assist visual comparison. Each panel shows experimental I(Q)s (symbols) at a series of [NCP]s as indicated in the legends, together with their respective theoretical fits (lines). The residues are shown with an offset at the same scale. The pertinent pair-potential parameters are (discussed in detail in the main text), (a) Z_{eff} = 22(1) e, σ=130 Å; (b) Z_{eff} = 21(1) e, σ=110 Å; (c) Z_{eff}=23(1) e, σ=130 Å; (d) Unreliable fitted values due to the relative low [NCP]s and thus not given.

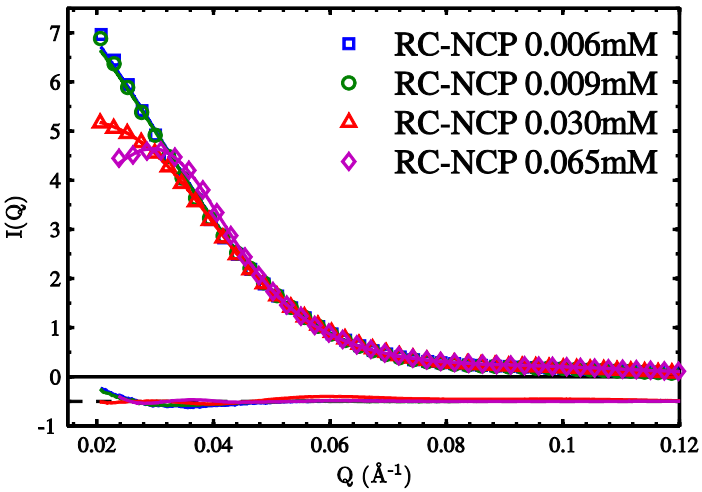

Figure S5. SAXS profiles and GOCM fits of intact recombinant RC-NCPs in 10 mM KCl. Annotations follow that of Fig. S4. The pair-potential parameters are, Z_{eff} =21(1) e, σ=140 Å.

II. Modeling the structure factor with a two-DH inter-NCP interaction potential

In addition to the use of either repulsive or attractive Debye-Huckel (DH) potential to fit the structure factor as in the main text, the inclusion of both DH terms in the inter-NCP potential was presented here. This potential takes the form below (the same as in the main text),

$$U(r)=\begin{cases}\infty & r<\sigma \\ \dfrac{Z_{eff}^2}{\varepsilon(1+\kappa\sigma/2)^2}\dfrac{e^{-\kappa(r-\sigma)}}{r}-\dfrac{Z_{attr}^2}{\varepsilon(1+\kappa_{attr}\sigma/2)^2}\dfrac{e^{-\kappa_{attr}(r-\sigma)}}{r} & r\geq\sigma\cdot\end{cases}$$

Here the hard-core potential has a fixed diameter of σ=100 Å for all samples; the electrostatic repulsive DH term has Debye length (1/κ) given by the ionic strength; and the attractive DH has decay length ($1/\kappa_{attr}$) fixed as 4.8 Å, equivalent to the Debye length at 400 mM monovalent salt. It should be noted that, as we don't know the exact nature of the inter-NCP attraction, the choice of a DH potential for inter-NCP attraction is convenient due to the available computational methods [2] but somewhat arbitrary. The choice of 4.8 Å Debye length is due to the most likely short-range nature of inter-NCP attraction, the observation of inter-molecular attractions of 4.8 Å decay length between various types of molecular surfaces[3], and the necessity of significant differences from the Debye length of the repulsive DH term in salt conditions from 10 to 200 mM KCl.

This leaves two fitting parameters in the inter-NCP potential, the effective charges of the repulsive (Z_{eff}) and attractive (Z_{attr}) DH terms. However, one complication is that there exists significant correlation between the two fitting parameters, particularly at high salts when their Debye lengths are close. This is because of the mutual cancellation effects of the two potentials. For this reason, while excellent fits were obtained (not shown), correlations between Z_{eff} and Z_{attr} values were evident from their fluctuations from sample to sample. To avoid such large fluctuations and facilitate comparisons between different salt conditions, we made one assumption that the attractive potential for each NCP construct (i.e., NS, gH3, or gH4 NCP) is independent of ion condition, i.e., the same Z_{attr} used for all salt conditions. The Z_{attr} value for each construct was determined by averaging the fitted Z_{attr} values at different salts for the particular construct. This procedure led to decreases of the fitting qualities, though rather satisfactory agreements with experimental data were obtained for all samples.

We show the fitted results based on the procedure discussed above in Figures S6-9 and the fitted potential parameters in Table S1. Compared with the fits with one DH-term potential discussed in the main text, the decrease of fitting quality is more significant for the more concentrated NCP samples. As the attractive DH term is present at all salt conditions, the fitted repulsive effective charges, Z_{eff}, are larger than those obtained with the one-DH repulsive potential as expected. The effective charges (<50 e) are still substantially smaller than the bare charge (~150 e) or the theoretical renormalized charges (>100 e). Qualitative comparisons are thus unchanged, while the fitted inter-NCP potentials are changed quantitatively as given in Table S1. For the attractive DH term, this fitting procedure obtains the effective charge Z_{attr} of 200, 165, and 154 e for the NS, gH3, and gH4 NCPs respectively. This is consistent with the results from one-DH potential fits indicating decreased attraction with tail deletions.

Overall, the inclusion of a persisting attractive term is intellectually pleasing as inter-NCP attraction (e.g., mediated by histone tails) is very likely present at all times, though overwhelmed by electrostatic repulsion at low salts. However, simultaneous determinations of both repulsive and attractive contributions are challenging.

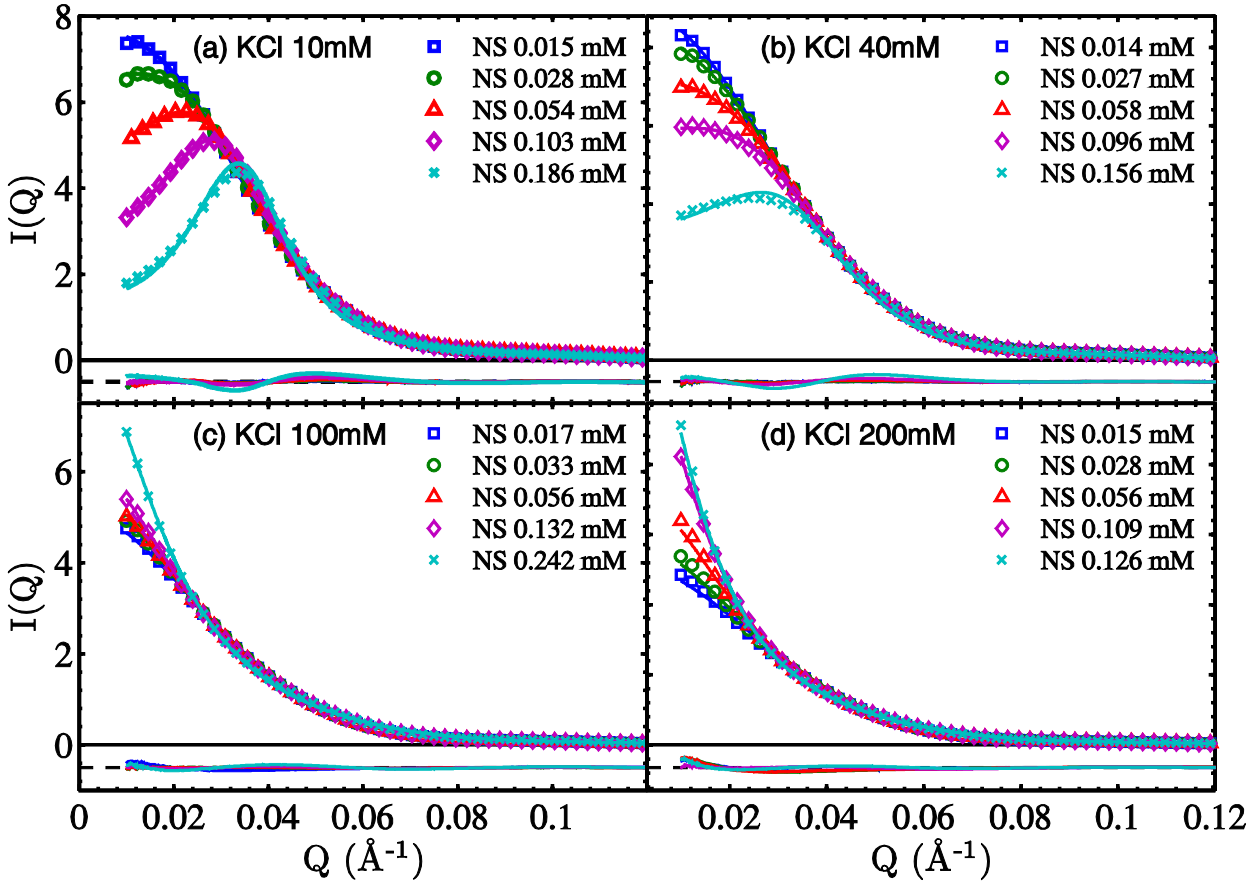

Figure S6. SAXS profiles of NS-NCP at four KCl concentrations together with fits based on the two-DH inter-NCP potential. Annotations are the same as in Fig. 2 in the main text.

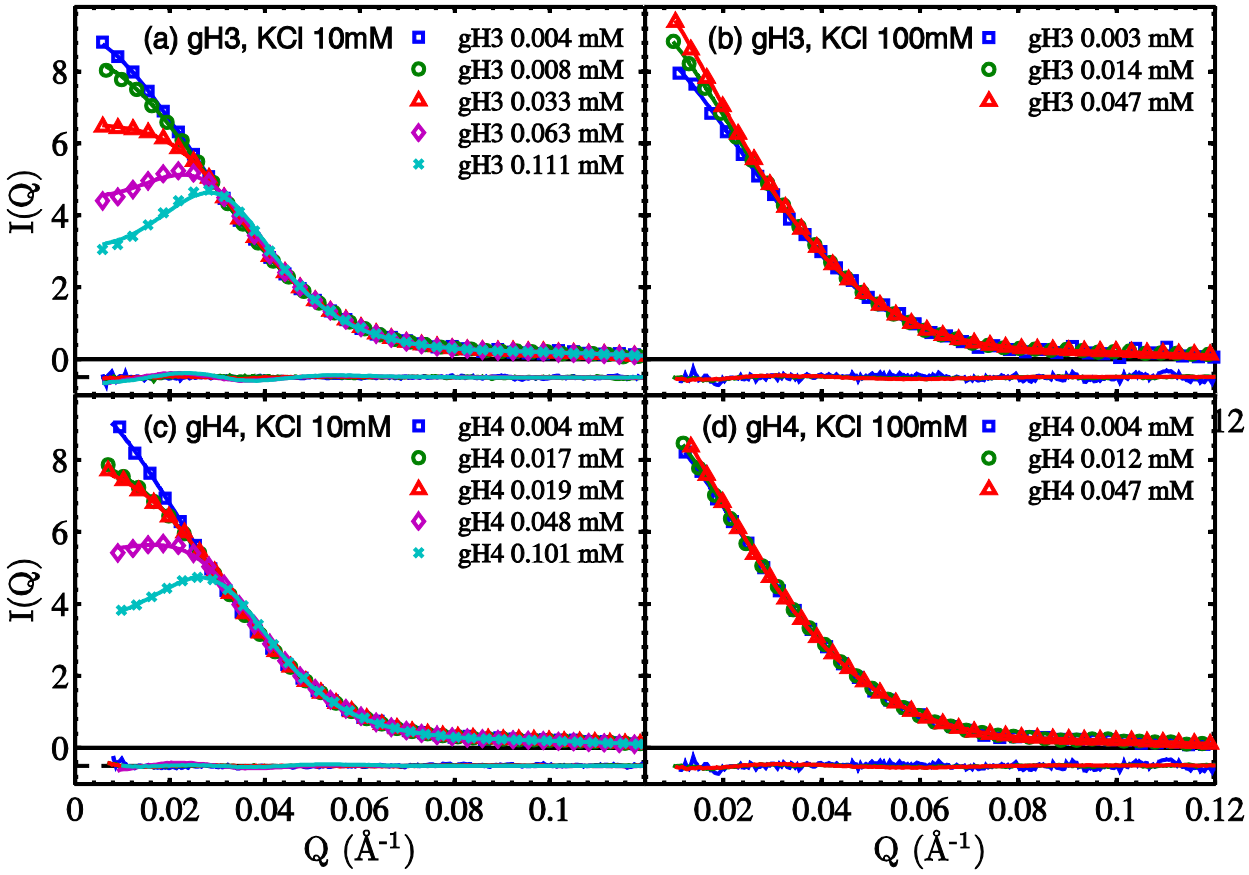

Figure S7. SAXS profiles of gH3 and gH4 NCPs at 10 and 100 mM KCl together with fits based on the two-DH inter-NCP potential. Annotations are the same as in Fig. 3 in the main text.

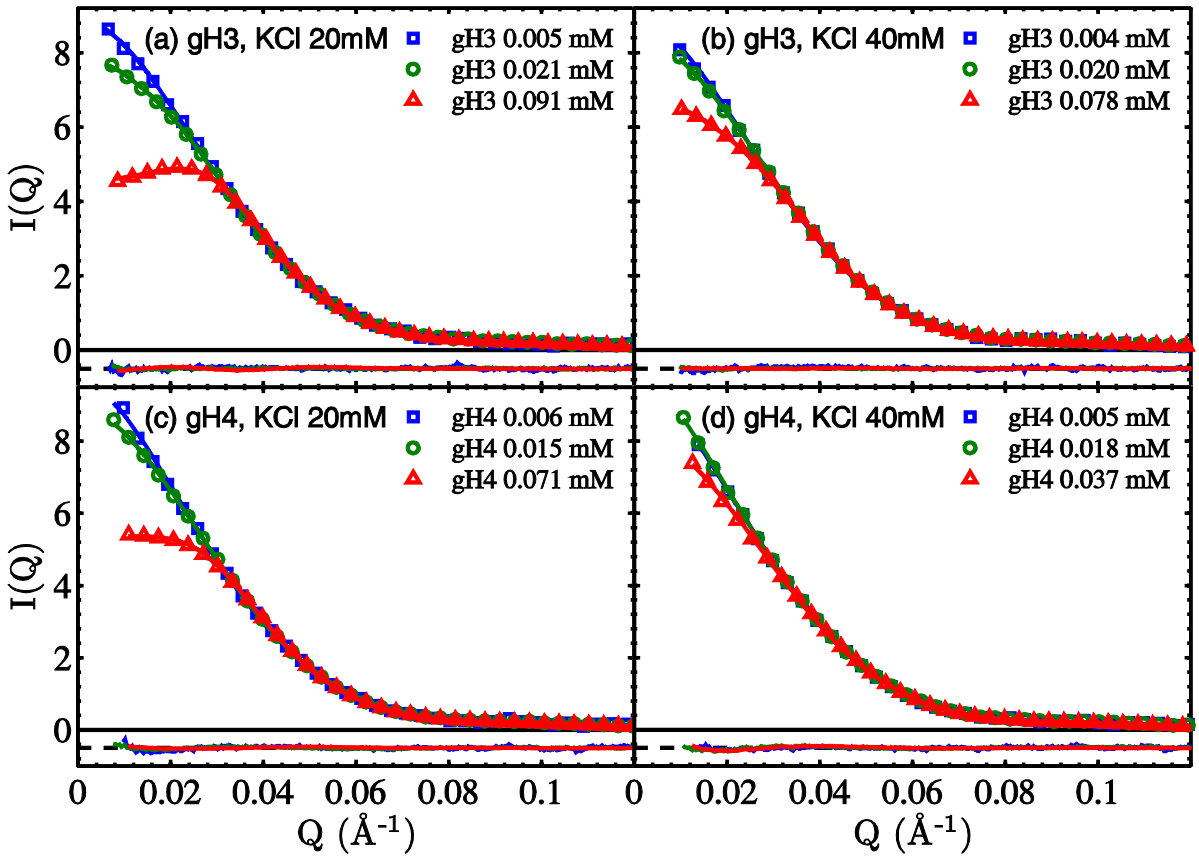

Figure S8. SAXS profiles of gH3 and gH4 NCPs at 20 and 40 mM KCl together with fits based on the two-DH inter-NCP potential.

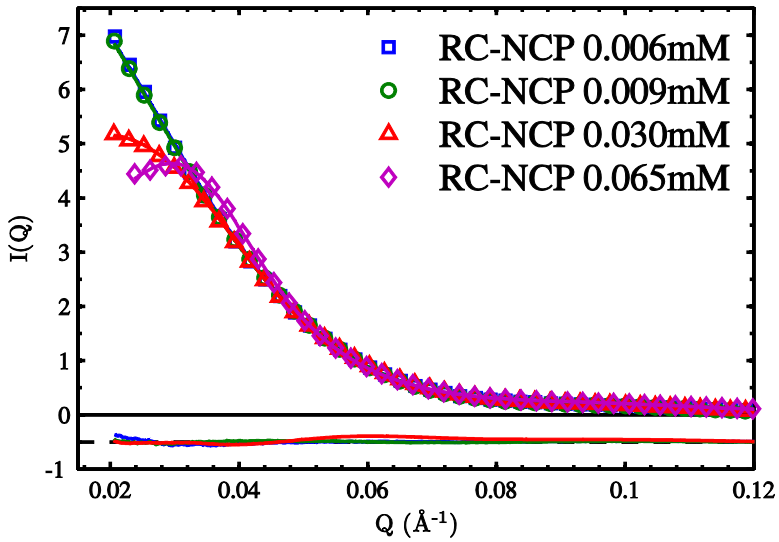

Figure S9. SAXS profiles of RC-NCPs at 10mM KCl together with fits based on the two-DH inter-NCP potential.

Table S1. Inter-NCP interaction parameters from structure factor fittings with either one-DH potential (in the main text) or two-DH potential (in the Supplemental Data). As the structure factors are more pronounced at high NCP concentrations, the values in this Table are taken as the mean over the 2-3 most concentrated samples for which the fits are the most reliable. For the fits with one DH term in the inter-NCP potential, the fitted effective charge (Z_{eff} or Z_{attr}) shows no systematic trends with the NCP concentration. For the fits with two DH terms, the fitted effective charge (Z_{eff}) generally increases slightly with the increase of the NCP concentration. We do not know the reason for the different trends from fitting the same data and speculate that this may arise from how the generalized one component method handles the effects of sample concentration with or without an attractive term [4]. Note the values for the gH4-NCP construct at 40 mM KCl are unreliable due to the relative low [NCP]s.

		One-DH inter-NCP potential			Two-DH inter-NCP-potential		
NCP construct	[KCl] (mM)	σ (Å)	Z_{eff} (e)	Z_{attr} (e)	σ (Å)	Z_{eff} (e)	Z_{attr} (e)
NS-NCP	10	140	22(1)	0	100	35(4)	200
	40	110	23(1)	0	100	49(6)	200
	100	100	0	150(5)	100	45(8)	200
	200	100	0	200(8)	100	1(1)	200
gH3-NCP	10	140	21(1)	0	100	31(3)	165
	20	130	22(1)	0	100	38(3)	165
	40	110	21(1)	0	100	48(4)	165
	100	100	0	123(4)	100	23(4)	165
gH4-NCP	10	140	20(1)	0	100	30(3)	154
	20	130	23(1)	0	100	33(3)	154
	40	--	--	--	--	--	--
	100	100	0	100(4)	100	30(10)	154
RC-NCP	10	140	21(1)	0	100	34(3)	200

1. Svergun D, Barberato C, Koch MHJ. *Crysol - a Program to Evaluate X-Ray Solution Scattering of Biological Macromolecules from Atomic Coordinates*. **J Appl Crystallogr**. 1995;28:768-73.
2. Liu Y, Chen W-R, Chen S-H. *Cluster Formation in Two-Yukawa Fluids*. **The Journal of Chemical Physics**. 2005;122(4):044507.
3. Zemb T, Parsegian VA. *Editorial Overview: Hydration Forces*. **Current opinion in colloid & interface science**. 2011;16(6):515-6. PMID: ISI:000298523900009.
4. Chen SH, Sheu EY, Kalus J, Hoffmann H. *Small-Angle Neutron-Scattering Investigation of Correlations in Charged Macromolecular and Supramolecular Solutions*. **J Appl Crystallogr**. 1988;21:751-69.